Pramod S. Phatak,[a] Bhaurao P. Sathe,[a] Sambhaji T. Dhumal,[c] Naziya N. M. A. Rehman,[b] Prashant P. Dixit,[b] Vijay M. Khedkar,[d] and Kishan P. Haval[a]*

[a]Department of Chemistry, Dr. B. A. M. U. Sub-Campus, Osmanabad, Maharashtra, India
[b]Department of Microbiology, Dr. B. A. M. U. Sub-Campus, Osmanabad, Maharashtra, India
[c]Department of Chemistry, Dr. B. A. M. U. Aurangabad, Aurangabad, Maharashtra, India
[d]Department of Pharmaceutical Chemistry, Shri Vile Parle Kelavani Mandal's Institute of Pharmacy, Dhule, Maharashtra, India
*E-mail: havalkp@gmail.com
Received October 25, 2018
DOI 10.1002/jhet.3568
Published online 31 May 2019 in Wiley Online Library (wileyonlinelibrary.com).

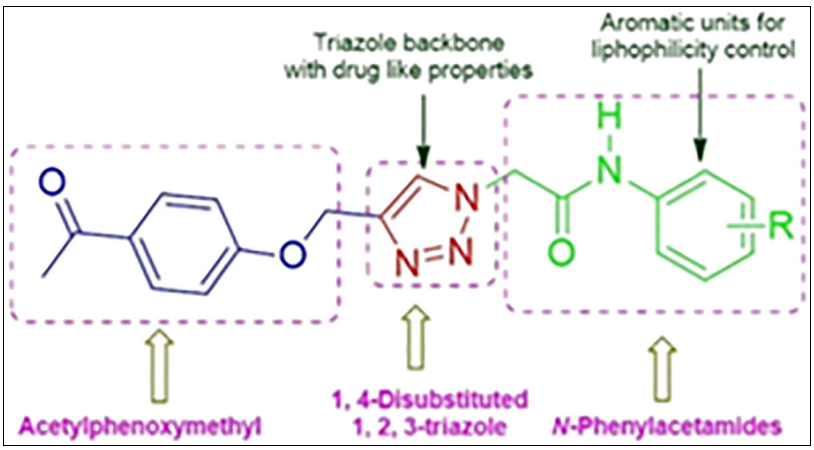

A series of molecules containing acetylphenoxymethyl, triazole, and *N*-phenylacetamide moieties were synthesized *via* the click chemistry approach. All the synthesized compounds were screened for their antimicrobial activities *in vitro*. The synthesized compounds **8a**, **8b**, **8m**, and **8n** showed better activities. We further performed exploratory docking studies to gain some insight regarding the molecular mechanism of antibacterial action of these compounds that could guide further structure-activity relationship (SAR) studies. We examined the interaction of the most active compound with DNA gyrase (pdb id:1KZN). Based on antimicrobial and docking studies, the compounds **8a**, **8b**, **8m**, and **8n** were identified as potential antimicrobial agents.

J. Heterocyclic Chem., **56**, 1928 (2019).

INTRODUCTION

Antimicrobials have been used to save the human population from the threat of infectious diseases. The emergence of microbial resistance is a significant health issue worldwide [1]. To counteract antimicrobial resistance, discovery of novel antimicrobial agents is one of the major medical concerns of the 21stcentury [2]. In this regard, many attempts were made to discover potential antimicrobial agents [3]. Triazoles are important five-membered heterocyclic scaffolds due to their extensive biological activities [4]. This framework can be readily obtained through click chemistry [5]. Literature revealed some triazole-based acetophenone derivatives shows antifungal and antioxidant activities [6]. Recently, Wang et al. reported a novel triazine-triazole derivatives as potential α-glucosidase inhibitors [7]. *N*-phenylacetamide or phenoxy acid coupling derivatives with anticancer [8], antiviral [9], antitubercular [10], antiinflammatory [11], hypoglycemic [12], antibacterial [13], antioxidant [14], and multidrug resistance reversing [15] activities are reported in literature. Bali et al. reported acetophenone-based piperazine derivatives as potential antipsychotics [16].

From earlier references, it is clear that acetylphenoxymethyl, triazole, or *N*-phenylacetamide coupling structures show considerable varied activities [17] (Fig. 1). Considering these facts and in continuation with our work on synthesis of bioactive compounds [18], herewith, we have reported new compounds with acetylphenoxymethyl, triazole, and *N*-phenylacetamide coupling structures and antimicrobial activities.

RESULTS AND DISCUSSION

Chemistry. Our convergent synthesis strategy starts with the preparation of 1-(4-(prop-2-ynyloxy)phenyl) ethanone (**3**) from *p*-hydroxy acetophenone (**1**) and

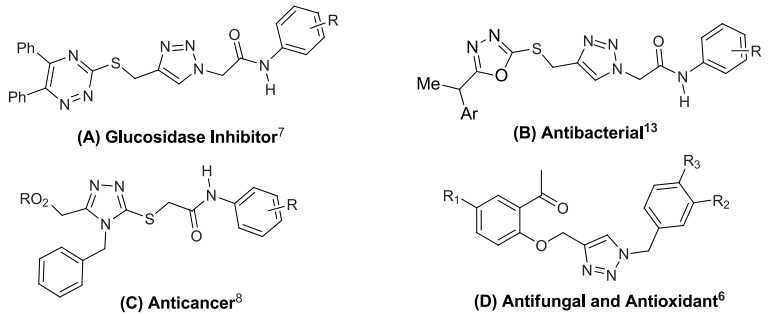

Figure 1. Some bioactive compounds having acetylphenoxymethyl, triazole, or *N*-phenylacetamide core structures.

Scheme 1. Synthesis of 1-(4-(prop-2-ynyloxy)phenyl)ethanone.

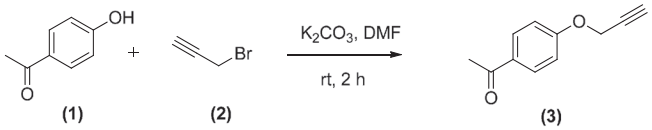

Scheme 2. Synthesis of substituted 2-azido-*N*-phenylacetamides.

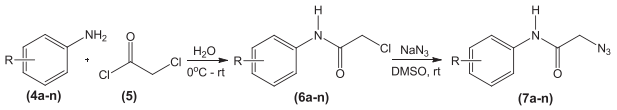

propargyl bromide (**2**) in the presence of potassium carbonate (Scheme 1). The substituted 2-chloro-*N*-phenylacetamides (**6a**–**n**) were prepared by reaction of substituted amines (**4a**–**n**) with acetyl chloride (**5**) in aqueous medium. Then, the obtained substituted 2-chloro-*N*-phenylacetamides (**6a**–**n**) were reacted with sodium azide in dimethyl sulfoxide (DMSO) at room temperature to furnish the corresponding substituted 2-azido-*N*-phenylacetamides (**7a**–**n**) (Scheme 2) [7a, 19]. Finally, click reaction of 1-(4-(prop-2-ynyloxy)phenyl) ethanone (**3**) with substituted 2-azido-*N*-phenylacetamides (**7a**–**n**) in the presence of copper sulfate pentahydrate and sodium ascorbate in PEG 400 at room temperature furnished the substituted acetylphenoxymethyl-triazolyl-*N*-phenylacetamides (**8a**–**n**) with 75–85% yields (Scheme 3). The series of compounds prepared with acetylphenoxymethyl, triazole, and *N*-phenylacetamide core structures are shown in Table 1. The structures of all the compounds obtained were confirmed by IR, ^{1}H-NMR, ^{13}C-NMR, and HRMS analytical techniques.

Biology. ***Antibacterial and antifungal activity.*** The synthesized compounds were tested for the antibacterial and antifungal activity. Both Gram-positive and Gram-negative bacterial pathogens were used in the antibacterial activity assay. *Staphylococcus aureus* ATCC 6538, *Bacillus cereus* ATCC 14579, *Bacillus megaterium* ATCC 2326, *Micrococcus glutamicum*, and *Bacillus subtilis* ATCC 6633 were Gram-positive pathogens used for this study. *Escherichia coli* ATCC 8739, *Salmonella typhi* ATCC 9207, *Shigella boydii* ATCC 12034, *Enterobacter aerogenes* ATCC 13048, *Pseudomonas aerogenosa* ATCC 9027, and *Salmonella abony* NCTC 6017 were the Gram-negative pathogens used in this study. Antifungal activity of synthesized compounds were determined against *Aspergillus niger* ATCC 16404, *Saccharomyces cereviseae* ATCC 9763, and *Candida albicans* ATCC 10231 fungal pathogens. Fluconazole and tetracycline were used as antifungal and antibacterial standard reference compounds, respectively. The antimicrobial activity of the compound was determined by agar well diffusion method as described by Mancini et al. with some modifications [20]. Synthesized compounds were dissolved in DMSO. Compounds solution was used at concentration of 2 μg/mL. Each bacterium and fungi was inoculated into sterile Nutrient broth medium and kept at 37°C for 24 h for developing

Scheme 3. Synthesis of substituted acetylphenoxymethyl-triazolyl-*N*-phenylacetamides

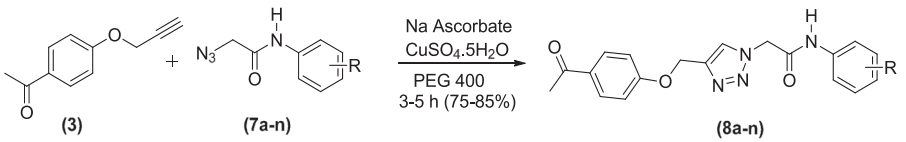

Table 1

Synthesis of substituted acetylphenoxymethyl-triazolyl-*N*-phenylacetamides.

Entry	Substituted 2-azido-*N*-phenylacetamides (**7a–n**)	Substituted acetylphenoxymethyl-triazolyl-*N*-phenylacetamides (**8a–n**)	Time (h)	% Yield
1	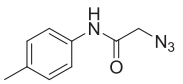	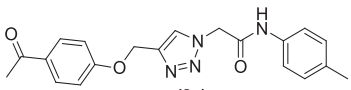 **(8a)**	3	82
2	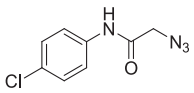	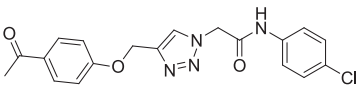 **(8b)**	4.5	78
3	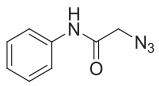	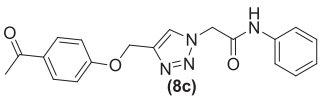 **(8c)**	4	80
4	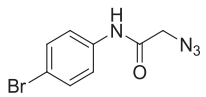	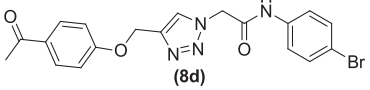 **(8d)**	4.5	84
5	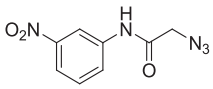	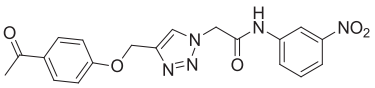 **(8e)**	5	75
6	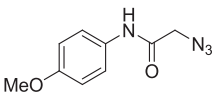	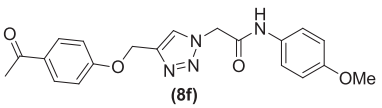 **(8f)**	3	85
7	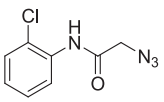	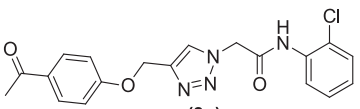 **(8g)**	4	76
8	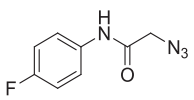	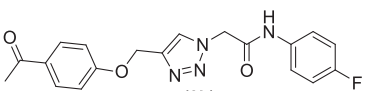 **(8h)**	4.5	82
9	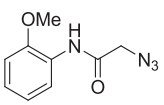	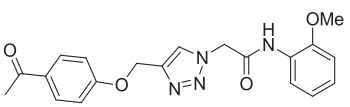 **(8i)**	4	84
10	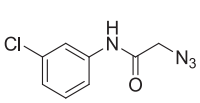	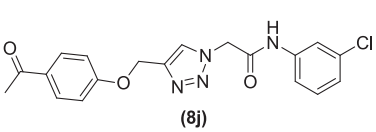 **(8j)**	4.5	78
11			3	81

(*Continues*)

Table 1

(*Continued*)

Entry	Substituted 2-azido-*N*-phenylacetamides (**7a–n**)	Substituted acetylphenoxymethyl-triazolyl-*N*-phenylacetamides (**8a–n**)	Time (h)	% Yield
	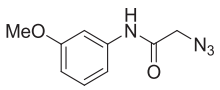	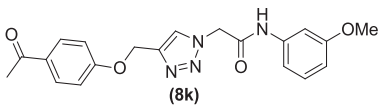 **(8k)**		
12	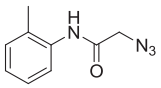	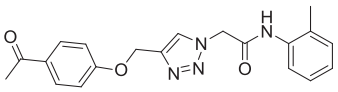 **(8l)**	3	82
13	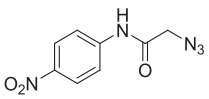	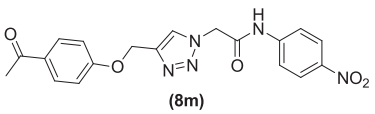 **(8m)**	5	75
14	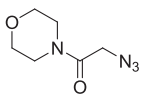	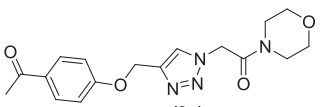 **(8n)**	4	76

inoculums, and then this broth was used for the study. Using sterile saline, the bacterial suspension was diluted to adjust the turbidity to the 0.5 McFarland standards; 200 μL diluted suspension of each pathogen was inoculated on sterile Mueller Hinton agar plates. Wells were made in the agar medium. Using micropipette, 100 μL of the each compound solution was put in a separate well. One hundred microliters of DMSO solution without any compound was also placed in a well to check its activity against the pathogenic culture. All Petri dishes were incubated for 24 h at 37°C. A clear zone around the well was considered as positive results. After complete incubation, the antimicrobial activity of the synthesized compounds was measured. Zones were measured and recorded by using scale in millimeters (mm). Out of 14 synthesized compounds, four compounds (**8a**, **8b**, **8m**, and **8n**) showed very good antimicrobial activity (Table 2), and therefore, these compounds minimum

Table 2

Results of antimicrobial assay of synthesized compounds against potent pathogens.

Compounds → Pathogens ↓	**8a**	**8b**	**8c**	**8d**	**8e**	**8f**	**8g**	**8h**	**8i**	**8j**	**8k**	**8l**	**8m**	**8n**	Standard*
S. typhi ATCC9207	13	12	07	-	-	-	-	-	-	-	-	-	16	12	27
E. aerogenes ATCC13048	07	07	-	-	-	-	-	-	06	-	-	-	10	09	33
B. subtilis ATCC 6633	11	14	-	09	-	08	-	10	-	10	-	-	15	14	34
C. albicans ATCC10231	-	12	-	10	-	-	-	-	-	-	-	-	08	08	25
P. aerogenosa ATCC9027	10	12	06	-	-	-	-	-	-	-	-	-	11	13	30
S. abony NCTC6017	08	12	-	-	-	-	-	-	-	-	-	-	11	16	30
B. megaterium ATCC 2326	08	11	-	-	-	-	-	-	-	-	-	-	12	-	27
E. coli ATCC8739	19	14	13	06	-	-	-	07	-	-	-	-	14	18	29
S. aureus ATCC 6538	15	12	15	-	-	-	-	-	-	11	08	-	13	17	25
S. boydii ATCC 12034	08	11	07	-	-	08	-	-	-	-	-	-	-	-	27
S. cerevisiae ATCC 9763	11	16	-	-	--	-	-	-	-	-	-	-	13	12	24
A. niger ATCC 16404	10	-	-	-	-	-	-	-	-	-	--	-	10	10	26
B. cereus ATCC 14579	13	11	-	07	10	-	--	-	-	-	10	-	12	12	33
M. glutamicus	09	16	-	-	08	-	-	-	-	-	-	-	05	07	31

Diameter of zone of inhibition is given in millimeters (mm).
*Standard used for antibacterial and antifungal activity was Tetracycline and Fluconazol, respectively.

Table 3

MIC values of most potent compounds.

Compounds → Pathogens ↓	**8a**	**8b**	**8m**	**8n**	Standard
S. typhi ATCC9207	140.0 ± 0.288	165.5 ± 1.040	85.0 ± 0.0	180.0 ± 0.577	3.0 ± 1.527
E. coli ATCC8739	55.5 ± 0.288	160.0 ± 0.577	135.0 ± 1.00	60.0 ± 0.0	4.5 ± 1.258
S. cerevisiae ATCC 9763	120.0 ± 1.154	110.0 ± 1.527	130.0 ± 0.50	115.0 ± 0.577	13 ± 1.154

inhibitory concentration was determined. Compound **8b** showed a good inhibitory activity against *S. cereviseae* ATCC 9763.

Minimum inhibitory concentration (MIC). Minimum inhibitory concentration (MIC) is the lowest concentration of an antimicrobial (compounds) drug that will inhibit the visible growth of a microorganism after overnight incubation. The MIC was determined for the most potent selected four compounds (**8a**, **8b**, **8m**, and **8n**). The MIC was determined against *E. coli* ATCC 8739, S. cerevisiae ATCC 9763, and *S. typhi* ATCC 9207. The MIC was determined by following the method and guidelines of Clinical and Laboratory Standard Institute. The results are shown in Table 3. The compound **8n** was found to inhibit the visible growth of *E. coli* ATCC 8739 at low concentration with MIC 60.0 μg/mL. All experiments were performed in triplicates and results are expressed as mean ± SD in microgram per milliliter.

Molecular docking study. Molecular docking study was carried out to provide insights into the molecular binding modes of most active molecules (**8a**, **8b**, **8m**, and **8n**) inside the active site of a crucial antimicrobial target DNA gyrase. The technique involves mainly enzyme 3D structure selection and preparation, identification and assignment of active site (grid generation), ligand 3D structure preparation and optimization, and docking and analysis of docking results (binding affinity). The Glide (grid-based ligand docking with energetics) module included in the Small Drug Discovery Suite of Schrödinger molecular modeling software (Schrödinger, LLC, New York, NY, 2015) was used to do the molecular docking study [21]. With this purpose, the 3D crystal structure of DNA gyrase subunit b in complex with an inhibitor (Protein with Accession number: 1KZN) was obtained from the RCSB Protein Data Bank (http://www.rcsb.org/pdb/). Firstly, the enzyme structure was imported, optimized, and minimized by removing unwanted molecules and other defects reported by the software using its *Protein Preparation Wizard*. Finally, a low energy minimized enzyme structure was obtained and used for further docking studies. Energy minimized enzyme structure was used to define the shape and properties of active site (grid generation) using Receptor Grid Generation panel in Glide which involves selected ligand as the reference (the co-crystallized ligand in the Protein DataBank (PDB) file) as it signifies the binding sites of drug with respect to the target. The generated grid was used for further docking of new molecules. A grid box of 12 × 12 × 12 Å dimensions centered on the centroid of the co-crystallized ligand was generated to define the active site which was large enough to explore the enzyme surface and identify the correct binding mode. The 3D structures of were generated and optimized using *ligand preparation* module of Schrodinger suite and subjected to docking simulation against the defined active site of the enzyme. The Glide extra precision (i.e., GlideXP) scoring function was used to measure their binding affinities. The output files, that is, docking poses generated in the form of docking poses were visualized to examine spatial fit of the ligand in the active site and investigated for the crucial elements of interaction (bonded and non-bonded) with the active site residues using the Maestro's Pose Viewer utility.

The level of antibacterial activities demonstrated by the title compounds prompted us to elucidate the plausible of mechanism of action for the title compounds. The *Molecular modeling* approach of molecular docking has emerged as an integral component of the drug discovery process to predict, with a substantial level of accuracy, the conformation of ligands within the target active site and also imparts knowledge on the ligand–protein interactions that govern the observed biological activity. With this objective molecular docking, study was carried out for the title compounds against a crucial antibacterial target-DNA gyrase subunit b (pdb id:1KZN), inhibition of which blocks relaxation of supercoiled DNA, relaxation being a requirement for transcription and replication. Owing to a critical role in bacterial cell survival and lack of this enzyme in higher eukaryotes, the bacterial DNA gyrase has been exploited as an antibacterial target. However, overzealous use of gyrase inhibitors such as fluoroquinolones is imposing a selective pressure on bacteria and drives the evolution of multidrug resistance in many pathogens [22]. All the four active compounds (**8a**, **8b**, **8m**, and **8n**) were docked very well into the active site of DNA gyrase producing an average docking score of −8.387 and binding energy

Table 4

The per-residue interaction analysis of substituted acetylphenoxymethyl-triazolyl-*N*-phenylacetamides in the active site of *DNA gyrase subunit b*.

Code	*Antimicrobialactivity* (MIC μg/mL)			Docking score	Glide interaction energy (kcal/mol)	Per-residues interactions		
	S. typhi	*E. coli*	*S. cerevisiae*			Van der Waals (kcal/mol)	Coulombic (kcal/mol)	H-bonds (Å)
8a	140	55	120	−8.462	−48.434	Val167(−1.884), Met166(−1.983), Thr165(−2.775), Arg136(−1.969), Val120(−1.694), Ile90(−3.239), Pro79(−3.225), Ile78(−3.696), Arg76(−3.831), Asp73(−1.224), Gln72(−1.039), Val71(−1.647), Glu50(−1.509), Ala47(−1.581), Asn46(−3.257), Val43(−1.926)	Arg136 (−2.163), Asp74 (−1.441), Asp73 (−1.476), Asn46 (−1.061)	Arg136(1.94), Arg136(2.77)
8b	165	160	110	−8.484	−47.473	Val167(−1.857), Met166(−1.879), Thr165(−3.311), Arg136(−1.024), Val120(−1.632), Ile90(−3.282), Pro79(−3.233), Ile78(−3.831), Arg76(−3.939), Asp73(−1.67), Gln72(−1.001), Val71(−1.531), Glu50(−1.514), Ala47(−1.909), Asn46(−3.275), Val43 (−1.997)	Arg136 (−2.567), Asp74 (−1.513), Asp73 (−1.762), Asn46 (−1.205),	Arg136(1.96), Arg136(2.76)
8m	85	135	130	−8.529	−48.221	Val167(−2.345), Met166(−1.025), Thr165(−3.403), Val120(−1.029), Ile90(−2.644), Pro79(−3.896), Ile78(−3.343), Arg76(−3.31), Asp74(−1.661), Asp73(−1.741), Gln72(−1.242), Val71(−1.992), Glu50(−1.713), Ala47(−2.444), Asn46(−4.27), Val43(−2.335)	Arg136 (−2.377), Asp74 (−1.346), Asp73 (−1.756), Glu50 (−2.408), Asn46 (−2.464)	Asn46(2.28), Arg136(1.77)
8n	180	60	115	−8.073	−46.573	Val167(−2.284), Met166(−1.203), Thr165(−3.473), Arg136(−1.917), Val120(−1.143), Ile90(−2.941), Pro79(−2.872), Ile78(−4.496), Arg76(−2.931), Asp73(−1.945), Gln72(−1.157), Val71(−2.266), Glu50(−2.289), Ala47(−1.993), Asn46(−3.894), Val43(−2.218)	Arg136 (−2.177), Asp74 (−1.023), Asp73 (−1.937), Glu50 (−2.161), Asn46 (−1.226)	Asn46(2.28)
Chlorobiocin	-	-	-	−9.902	−50.733	Val167(−2.896), Met166(−1.934), Thr165(−3.788), Arg136(−1.951), Val120(−1.189), Ile90(−2.992), Pro79(−3.775), Ile78(−6.093), Gly77(−1.689), Arg76(−3.38), Asp73(−2.924), Gln72(−1.898), Val71(−2.239), Glu50(−3.071), Asp49(−1.592), Ala47(−2.525), Asn46(−4.711), Val43(−2.847),	Lys139(−1.502), Arg136(−3.801) Asp74(−1.836), Asp73(−1.779), Asn46(−4.776), Asp45(−2.008),	Arg136(2.69), Arg136(2.11) Asn46(2.90), Asn46(2.01) Asp73(2.19)

of −47.675 kcal/mol, while the docking score of reference standard clorobiocin was found to be −9.902 Glide energy of −50.733 kcal/mol. A detailed account of per-residue bonded and non-bonded interaction analysis with these molecules was carried out to determine the most significantly interacting residues and also their nature of interactions (Table 4). This analysis is discussed in detail for one of the most active compound (**8m**) in the next section.

The best scored docked conformation of **8m** could snugly fit into the active site of bacterial DNA gyrase engaging in a network of specific steric and electrostatic interactions and the binding is further stabilized by few prominent hydrogen bonding (Fig. 2).

The most significant steric interactions were observed through 2-(4-((4-acetylphenoxy)methyl) component of **8m** with Val167(−2.345 kcal/mol), Met166(−1.025 kcal/mol), Thr165(−3.403 kcal/mol), Asp74(−1.661 kcal/mol), Asp73(−1.741 kcal/mol), Val71(−1.992 kcal/mol), Glu50(−1.713 kcal/mol), Ala47(−2.444 kcal/mol), and Val43(−2.335 kcal/mol) residues while the 1*H*-1,2,3-triazol-1-yl) part of the

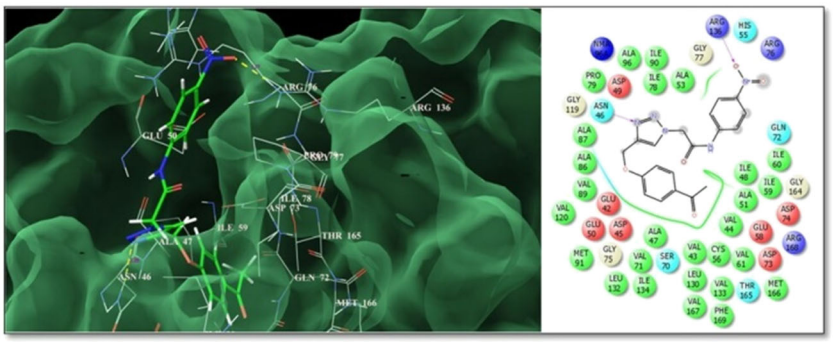

Figure 2. Binding mode of **8m** into the active site of *DNA gyrase subunit b* (on right side: the pink lines represent the hydrogen bonding interactions). [Color figure can be viewed at wileyonlinelibrary.com]

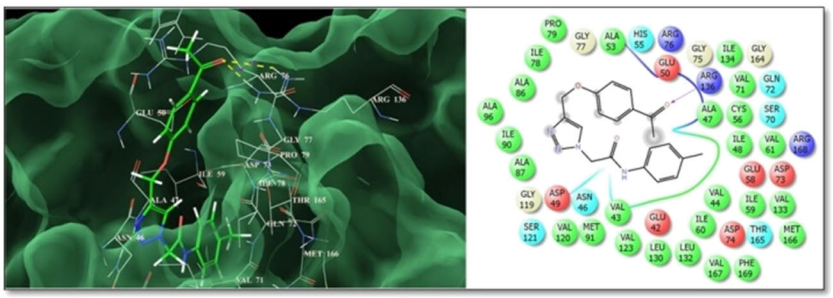

Figure 3. Binding mode of **8a** into the active site of *DNA gyrase subunit b* (on right side: the pink lines represent the hydrogen bonding interactions). [Color figure can be viewed at wileyonlinelibrary.com]

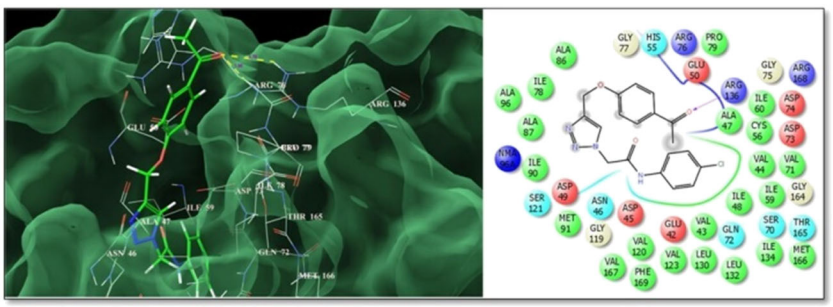

Figure 4. Binding mode of **8b** into the active site of *DNA gyrase subunit b* (on right side: the pink lines represent the hydrogen bonding interactions). [Color figure can be viewed at wileyonlinelibrary.com]

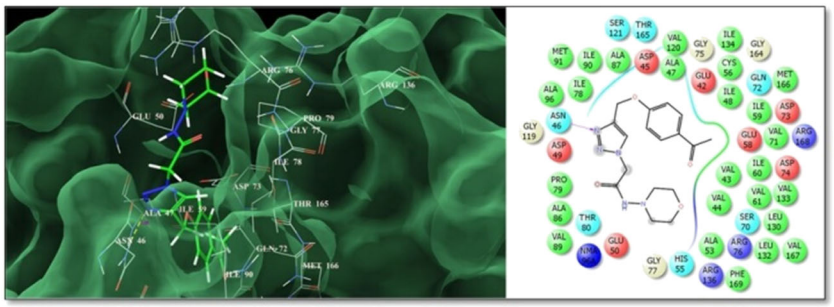

Figure 5. Binding mode of **8n** into the active site of *DNA gyrase subunit b* (on right side: the pink lines represent the hydrogen bonding interactions). [Color figure can be viewed at wileyonlinelibrary.com]

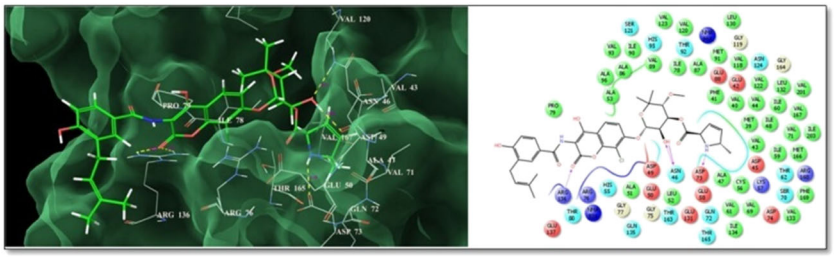

Figure 6. Binding mode of chlorobiocin into the active site of *DNA gyrase subunit b* (on right side: the pink lines represent the hydrogen bonding interactions). [Color figure can be viewed at wileyonlinelibrary.com]

molecule was seen to be engaged in similar interactions with Val120(−1.029 kcal/mol), Ile90(−2.644 kcal/mol), Pro79(−3.896 kcal/mol), Ile78(−3.343 kcal/mol), and Asn46(−4.27 kcal/mol) residues, and finally the *para-nitro*-phenylacetamides component showed interactions with Arg76(−3.31 kcal/mol) and Gln72(−1.242 kcal/mol) residues. The enhanced affinity towards the enzyme of **8m** is also attributed to favorable columbic interactions observed with Arg136(−2.377 kcal/mol), Asp74(−1.346 kcal/mol), Asp73(−1.756 kcal/mol), Glu50(−2.408 kcal/mol), and Asn46(−2.464 kcal/mol) residues of the active site of enzyme. Furthermore, the compound **8m** is observed to be engaged in a very prominent hydrogen bonding interactions, first with Asn46 residue through the nitrogen (-NH-) of the triazole scaffold and the second with Arg136 through the nitro (NO_2) group having bond distances of 2.28 and 1.77 Å, respectively. These hydrogen bonds anchor the ligand into the active site and aid the non-bonded interactions (steric and electrostatic) between the ligand and the enzyme. Similar networks of balanced steric and electrostatic non-bonded interactions as well as bonded interactions (hydrogen bond) were observed for other molecules (**8a**, **8b**, and **8n**) (Figs 3, 4, and 5). These per-residue interaction energies when compared to the standard clorobiocin show that the lower values observed for **8m** and other analogues (**8a**, **8b**, and **8n**) could probably be responsible for their lower antibacterial activity. These per-residue interaction energies were compared with the values of reference clorobiocin. This indicates that compound **8m** and other analogues (**8a**, **8b** and **8n**) probably less interacting with the target enzyme DNA Gyrase, and hence showing less antimicrobial activities. This binding affinity data and more specifically the per-residue ligand interaction analysis can be fruitfully utilized for the structure-based lead optimization of these derivatives to design potent and selective antibacterial agents with selectively improving the bonded and non-bonded (steric and electrostatic) interaction with the active site residues (Fig. 6).

CONCLUSIONS

In conclusion, we have synthesized novel substituted acetylphenoxymethyl-triazolyl-*N*-phenylacetamides. Among the synthesized compounds, four have been shown very good antibacterial and antifungal activity. Furthermore, molecular docking study could provide valuable insight into the plausible mechanism of antibacterial action demonstrated by these molecules. The per-residue interaction analysis could shed light onto the thermodynamic interactions guiding the orientation of these molecules into the active site of DNA gyrase. The information derived from the in silico binding affinity study is being utilized for the modification of the potential

antimicrobial agents in this study, and the results will be communicated in the future communication.

EXPERIMENTAL

Procedure for the synthesis of 1-(4-(prop-2-ynyloxy)phenyl) ethanone (3). A mixture of 4-hydroxyacetophenone (**1**) (0.01 mol) and propargyl bromide (**2**) (0.01 mol) in the presence of potassium carbonate (0.015 mol) was stirred in dimethylformamide at room temperature for 2 h. Then, the reaction mixture was poured on crushed ice and solid obtained was filtered. The product obtained was recrystallized in ethanol.

General procedure for the synthesis of substituted 2-azido-*N*-phenylacetamides (7a–n). The chloroacetyl chloride (**5**) (0.015 mol) was added dropwise in aqueous solution of substituted anilines (**4a–n**) (0.01 mol) at 0°C and stirred for 8–10 h at room temperature. The progress of reaction was monitored by thin-layer chromatography. After completion of reaction, the reaction mixture was poured on ice. The solid obtained were filtered and recrystallized with ethanol to furnish the corresponding substituted 2-chloro-*N*-phenylacetamides (**6a–n**). Then, the obtained substituted 2-chloro-*N*-phenylacetamides (**6a–n**) (0.01 mol) and sodium azide (0.01 mol) was stirred in DMSO for 5–6 h at room temperature. After completion of reaction, the water was added in reaction mixture and extracted with ethyl acetate to give the corresponding substituted 2-azido-*N*-phenylacetamides (**7a–n**).

General procedure for the synthesis of substituted acetylphenoxymethyl-triazolyl-*N*-phenylacetamides (8a–n). 1-(4-(Prop-2-ynyloxy)phenyl)ethanone (**3**) (0.01 mol) and substituted 2-azido-*N*-phenylacetamides (**7a–n**) (0.01 mol) were stirred in the presence of $CuSO_4.5H_2O$ (20 mol%) and sodium ascorbate (20 mol%) in PEG-400 at room temperature. The progress of the reaction was monitored by thin-layer chromatography. After completion of the reaction, the reaction mixture was poured on ice. The white solid obtained was filtered, washed with water, and recrystallized in ethanol.

2-(4-((4-Acetylphenoxy)methyl)-1H-1,2,3-triazol-1-yl)-N-p-tolylacetamide (8a). Yield: 82%; M.P.: 265°C; white solid; IR (Neat) ν cm^{-1}: 3208, 3077, 2980, 1695, 1670, 1600, 1556, 1508, 1419, 1286, 1217, 833, 821; ^{1}H-NMR (400 MHz, $CDCl_3$): δ 2.30 (s, 3H, -CH_3), 2.56 (s, 3H, -CH_3), 5.27 (s, 2H, -CH_2), 5.28 (s, 2H, -CH_2), 7.06 (d, J = 8 Hz, 2H, Ar-H), 7.10 (d, J = 8 Hz, 2H, Ar-H), 7.46 (d, J = 8 Hz, 2H, Ar-H), 7.94 (d, J = 8 Hz, 2H, Ar-H), 8.02 (s, 1H, 1,2,3-triazole-H), 10.07 (s, 1H, -NH); ^{13}C-NMR (75 MHz, $CDCl_3$ + DMSO-d_6): δ 20.3, 25.9, 52.4, 61.4, 105.9, 114.0, 119.4, 124.7, 128.8, 130.0, 133.3, 135.0, 142.5, 161.6, 162.9, 196.2; HRMS $(ESI)^+$ calcd for $C_{20}H_{20}N_4O_3$ $[M + H]^+$: 365.1569 and found 365.1615.

2-(4-((4-Acetylphenoxy)methyl)-1H-1,2,3-triazol-1-yl)-N-(4-chlorophenyl)acetamide (8b). Yield: 78%; M.P.: 310°C; white solid; IR (Neat) ν cm^{-1}: 3327, 1693, 1666, 1600, 1551, 1494, 1293, 1246, 1175, 1047, 837, 815; ^{1}H-NMR (300 MHz, $CDCl_3$ + DMSO-d_6): δ 2.55 (s, 3H, -CH_3), 5.28 (s, 2H, -CH_2), 5.31 (s, 2H, -CH_2), 7.09 (d, J = 9 Hz, 2H, Ar-H), 7.27 (d, J = 9 Hz, 2H, Ar-H), 7.60 (d, J = 9 Hz, 2H, Ar-H), 7.94 (d, J = 9 Hz, 2H, Ar-H), 8.10 (s, 1H, 1,2,3-triazole-H), 10.45 (s, 1H, -NH); ^{13}C-NMR (75 MHz, DMSO-d_6): δ 25.9, 28.9, 52.1, 61.2, 114.0, 120.5, 125.3, 127.9, 128.2, 130.0, 136.6, 142.1, 161.6, 163.4, 195.7; HRMS $(ESI)^+$ calcd for $C_{19}H_{17}ClN_4O_3$ $[M + H]^+$: 386.0960 and found 386.1096.

2-(4-((4-Acetylphenoxy)methyl)-1H-1,2,3-triazol-1-yl)-N-phenylacetamide (8c). Yield: 80%; M.P.: 220°C; grey solid; IR (Neat) ν cm^{-1}: 3271, 3094, 2917, 1670, 1599, 1542, 1314, 1174, 1038, 842, 817; ^{1}H-NMR (400 MHz, $CDCl_3$): δ 2.55 (s, 3H, -CH_3), 5.28 (s, 4H, -CH_2), 7.06 (d, J = 8 Hz, 2H, Ar-H), 7.11 (d, J = 8 Hz, 1H, Ar-H), 7.30 (t, J = 8 Hz, 2H, Ar-H), 7.58 (d, J = 8 Hz, 2H, Ar-H), 7.93 (d, J = 8 Hz, 2H, Ar-H), 8.02 (s, 1H, 1,2,3-triazole-H), 10.14 (s, 1H, -NH); ^{13}C-NMR (75 MHz, $CDCl_3$ + DMSO-d_6): δ 25.8, 52.3, 61.2, 113.9, 119.2, 123.7, 124.7, 128.3, 129.9, 137.5, 139.9, 142.4, 161.5, 163.0, 195.9; HRMS $(ESI)^+$ calcd for $C_{19}H_{18}N_4O_3$ $[M + H]^+$: 351.1412 and found 351.1425.

2-(4-((4-Acetylphenoxy)methyl)-1H-1,2,3-triazol-1-yl)-N-(4-bromophenyl)acetamide (8d). Yield: 84%; M.P.: 270°C; white solid; IR (Neat) ν cm^{-1}: 3299, 3161, 3065, 2996, 1663, 1599, 1493, 1247, 1174, 1047, 865, 856; ^{1}H-NMR (300 MHz, $CDCl_3$ + DMSO-d_6): δ 2.56 (s, 3H, -CH_3), 5.29 (s, 2H, -CH_2), 5.30 (s, 2H, -CH_2), 7.08 (d, J = 9 Hz, 2H, Ar-H), 7.41 (d, J = 9 Hz, 2H, Ar-H), 7.54 (d, J = 9 Hz, 2H, Ar-H), 7.94 (d, J = 9 Hz, 2H, Ar-H), 8.07 (s, 1H, 1,2,3-triazole-H), 10.42 (s, 1H, -NH); ^{13}C-NMR (75 MHz, $CDCl_3$ + DMSO-d_6): δ 25.9, 52.2, 61.2, 91.5, 113.9, 120.8, 124.9, 130.0, 131.1, 136.9, 142.2, 161.6, 163.2, 175.1, 195.8; HRMS $(ESI)^+$ calcd for $C_{19}H_{17}BrN_4O_3$ $[M + H]^+$: 430.0464 and found 431.0525.

2-(4-((4-Acetylphenoxy)methyl)-1H-1,2,3-trizol-1-yl)-N-(3-nitrophenyl)acetamide (8e). Yield: 75%; M.P.: 240°C; yellow solid; IR (Neat) ν cm^{-1}: 3291, 3163, 3099, 1660, 1598, 1526, 1349, 1254, 1181, 1050, 847, 824; ^{1}H-NMR (300 MHz, $CDCl_3$ + DMSO-d_6): δ 2.55 (s, 3H, -CH_3), 5.30 (s, 2H, -CH_2), 5.37 (s, 2H, -CH_2), 7.09 (d, J = 9 Hz, 2H, Ar-H), 7.53 (t, J = 9 Hz, 1H, Ar-H), 7.94 (d, J = 9 Hz, 4H, Ar-H), 8.13 (s, 1H, 1,2,3-triazole-H), 8.60 (s, 1H, Ar-H), 10.88 (s, 1H, -NH); ^{13}C-NMR (75 MHz, $CDCl_3$ + DMSO-d_6): δ 26.0, 52.1, 61.2, 113.6, 114.1, 118.0, 124.8, 124.9, 125.6, 129.5, 130.1, 139.2, 142.2, 147.9, 161.7, 164.3, 195.9; HRMS $(ESI)^+$ calcd for $C_{19}H_{17}N_5O_5$ $[M + H]^+$: 396.1263 and found 396.1301.

2-(4-((4-Acetylphenoxy)methyl)-1H-1,2,3-trizol-1-yl)-N-(4-methoxyphenyl)acetamide (8f). Yield: 85%; M.P.: 255°C; white solid; IR (Neat) ν cm^{-1}: 3270, 3087, 2917, 2848,

1670, 1599, 1251, 1174, 844, 823; ^{1}H-NMR (300 MHz, $CDCl_3$ + DMSO-d_6): δ 2.54 (s, 3H, -CH_3), 3.77 (s, 3H, -OMe), 5.28 (d, 4H, -CH_2), 6.84 (d, J = 9 Hz, 2H, Ar-H), 7.09 (d, J = 9 Hz, 2H, Ar-H), 7.51 (d, J = 9 Hz, 2H, Ar-H), 7.93 (d, J = 9 Hz, 2H, Ar-H), 8.14 (s, 1H, 1,2,3-triazole-H), 10.23 (s, 1H, -NH); ^{13}C-NMR (75 MHz, DMSO-d_6): δ 26.0, 35.8, 54.8, 61.9, 113.4, 114.0, 120.6, 125.4, 130.0, 131.0, 142.0, 155.5, 161.6, 161.8, 162.9, 195.7.

2-(4-((4-Acetylphenoxy)methyl)-1H-1,2,3-triazol-1-yl)-N-(2-chlorophenyl)acetamide (8g). Yield: 76%; M.P.: 200°C; white solid; IR (Neat) ν cm^{-1}: 3338, 2993, 1697, 1668, 1600, 1532, 1443, 1254, 1181, 1167, 1047, 842, 754; ^{1}H-NMR (300 MHz, $CDCl_3$ + DMSO-d_6): δ 2.55 (s, 3H, -CH_3), 5.29 (s, 2H, -CH_2), 5.45 (s, 2H, -CH_2), 7.08 (d, J = 6 Hz, 2H, Ar-H), 7.14 (t, J = 6 Hz, 1H, Ar-H), 7.27 (t, J = 6 Hz, 1H, Ar-H), 7.42 (d, J = 9 Hz, 1H, Ar-H), 7.90 (d, J = 9 Hz, 1H, Ar-H), 7.94 (d, J = 9 Hz, 2H, Ar-H), 8.12 (s, 1H, 1,2,3-triazole-H), 9.78 (s, 1H, -NH); ^{13}C-NMR (75 MHz, DMSO-d_6): δ 25.9, 52.6, 61.2, 114.0, 112.8, 124.5, 125.3, 125.7, 126.8, 129.0, 130.0, 133.7, 142.1, 154.4, 161.6, 164.0, 195.7.

2-(4-((4-Acetylphenoxy)methyl)-1H-1,2,3-triazol-1-yl)-N-(4-fluorophenyl)acetamide (8h). Yield: 82%; M.P.: 245°C; white solid; IR (Neat) ν cm^{-1}: 3329, 1689, 1665, 1660, 1560, 1509, 1252, 1215, 1178, 1047, 840, 812; ^{1}H-NMR (300 MHz, $CDCl_3$ + DMSO-d_6): δ 2.56 (s, 3H, -CH_3), 5.28 (s, 4H, -CH_2), 7.00 (t, J = 9 Hz, 2H, Ar-H), 7.07 (d, J = 9 Hz, 2H, Ar-H), 7.55–7.59 (m, 2H, Ar-H), 7.94 (d, J = 9 Hz, 2H, Ar-H), 8.03 (s, 1H, 1,2,3-triazole-H), 10.29 (s, 1H, -NH); **^{13}**C-NMR (75 MHz, $CDCl_3$ + DMSO-d_6): δ 25.9, 52.2, 61.3, 113.9, 114.7, 115.0, 120.9, 121.0, 124.7, 130.0, 133.7, 142.4, 161.6, 163.0, 196.0.

2-(4-((4-Acetylphenoxy)methyl)-1H-1,2,3-triazol-1-yl)-N-(2-methoxyphenyl)acetamide (8i). Yield: 84%; M.P.: 150°C; white solid; IR (Neat) ν cm^{-1}: 3326, 2916, 1693, 1667, 1597, 1536, 1460, 1251, 1224, 1170, 1045, 1034, 839, 745; ^{1}H-NMR (300 MHz, $CDCl_3$ + DMSO-d_6): δ 2.55 (s, 3H, -CH_3), 3.87 (s, 3H, -OMe), 5.28 (s, 2H, -CH_2), 5.39 (s, 2H, -CH_2), 6.91 (t, J = 6 Hz, 2H, Ar-H), 7.05 (d, J = 9 Hz, 2H, Ar-H), 7.08–7.11 (m, 1H, Ar-H), 7.93 (d, J = 9 Hz, 2H, Ar-H), 8.04 (s, 1H, 1,2,3-triazole-H), 8.13 (d, J = 9 Hz, 1H, Ar-H), 9.12 (s, 1H, -NH); ^{13}C-NMR (75 MHz, $CDCl_3$ + DMSO-d_6): δ 25.8, 52.6, 55.2, 61.3, 110.0, 113.9, 120.2, 120.4, 124.4, 124.6, 126.0, 130.0, 142.7, 148.3, 161.5, 162.9, 196.1.

2-(4-((4-Acetylphenoxy)methyl)-1H-1,2,3-triazol-1-yl)-N-(3-chlorophenyl)acetamide (8j). Yield: 78%; M.P.: 250°C; grey solid; IR (Neat) ν cm^{-1}: 3327, 3158, 2917, 2848, 1692, 1666, 1597, 1543, 1429, 1251, 1182, 1050, 1037, 843, 783; ^{1}H-NMR (300 MHz, $CDCl_3$ + DMSO-d_6): δ 2.56 (s, 3H, -CH_3), 5.28 (s, 2H, -CH_2), 5.29 (s, 2H, -CH_2), 7.07 (d, J = 9 Hz, 2H, Ar-H), 7.24 (t, J = 6 Hz, 1H, Ar-H), 7.42–7.50 (m, 2H, Ar-H), 7.75 (t, J = 2 Hz, 1H, Ar-H), 7.94 (d, J = 9 Hz, 2H, Ar-H), 8.01 (s, 1H, 1,2,3-triazole-H), 10.36 (s, 1H, -NH); ^{13}C-NMR (75 MHz, $CDCl_3$ + DMSO-d_6): δ 25.8, 52.2, 61.2, 113.9, 116.0, 117.2, 119.2, 123.5, 124.7, 129.4, 129.9, 133.6, 138.8, 142.4, 161.5, 163.3, 195.9.

2-(4-((4-Acetylphenoxy)methyl)-1H-1,2,3-triazol-1-yl)-N-(3-methoxyphenyl)acetamide (8k). Yield: 81%; M.P.: 160°C; brown solid; IR (Neat) ν cm^{-1}: 3261, 3077, 1670, 1598, 1551, 1491, 1362, 1261, 1233, 1165, 1043, 1033, 852, 833; ^{1}H-NMR (300 MHz, $CDCl_3$ + DMSO-d_6): δ 2.55 (s, 3H, -CH_3), 3.77 (s, 3H, -OMe), 5.28 (s, 4H, -CH_2), 6.65 (dd, J = 3 Hz & 9 Hz, 1H, Ar-H), 7.04–7.08 (m, 3H, Ar-H), 7.20 (t, J = 9 Hz, 1H, Ar-H), 7.34 (t, J = 2 Hz, 1H, Ar-H), 7.93 (d, J = 9 Hz, 2H, Ar-H), 8.02 (s, 1H, 1,2,3-triazole-H), 10.18 (s, 1H, -NH); ^{13}C-NMR (75 MHz, $CDCl_3$ + DMSO-d_6): δ 25.8, 52.4, 54.7, 61.3, 105.1, 107.2, 109.6, 111.5, 113.9, 124.5, 129.0, 130.0, 138.6, 142.6, 159.4, 161.5, 163.0, 196.1.

2-(4-((4-Acetylphenoxy)methyl)-1H-1,2,3-triazol-1-yl)-N-o-tolylacetamide (8l). Yield: 82%; M.P.: 200°C; white solid; IR (Neat) ν cm^{-1}: 3287, 3096, 2920, 1670, 1600, 1537, 1249, 1229, 1173, 1045, 961, 834, 815; ^{1}H-NMR (400 MHz, $CDCl_3$): δ 2.25 (s, 3H, -CH_3), 2.55 (s, 3H, -CH_3), 5.28 (s, 2H, -CH_2), 5.35 (s, 2H, -CH_2), 7.06 (d, J = 8 Hz, 2H, Ar-H), 7.12–7.20 (m, 2H, Ar-H), 7.51–7.59 (m, 2H, Ar-H), 7.93 (d, J = 8 Hz, 2H, Ar-H), 8.05 (s, 1H, 1,2,3-triazole-H), 9.48 (s, 1H, -NH); ^{13}C-NMR (75 MHz, $CDCl_3$ + DMSO-d_6): δ 17.4, 25.8, 52.1, 61.2, 113.9, 124.0, 124.6, 125.3, 125.7, 129.9, 130.0, 130.8, 134.5, 142.4, 148.8, 161.5, 163.3, 195.9.

2-(4-((4-Acetylphenoxy)methyl)-1H-1,2,3-triazol-1-yl)-N-(4-nitrophenyl)acetamide (8m). Yield: 75%; M.P.: 260°C; brown solid; IR (Neat) ν cm^{-1}: 3299, 1700, 1661, 1599, 1573, 1495, 1345, 1251, 1175, 1047, 855, 843, 821; ^{1}H-NMR (300 MHz, $CDCl_3$ + DMSO-d_6): δ 2.56 (s, 3H, -CH_3), 5.30 (s, 2H, -CH_2), 5.39 (s, 2H, -CH_2), 7.09 (d, J = 9 Hz, 2H, Ar-H), 7.84 (d, J = 9 Hz, 2H, Ar-H), 7.94 (d, J = 9 Hz, 2H, Ar-H), 8.11 (s, 1H, 1,2,3-triazole-H), 8.19 (d, J = 9 Hz, 2H, Ar-H), 10.93 (s, 1H, -NH); ^{13}C-NMR (75 MHz, $CDCl_3$ + DMSO-d_6): δ 25.8, 52.3, 61.3, 113.9, 118.8, 124.2, 124.6, 129.9, 142.8, 143.6, 157.2, 161.8, 163.8, 185.1, 196.0; HRMS (ESI)$^+$ calcd for $C_{19}H_{17}N_5O_5$ [M + H]$^+$: 396.1263 and found 396.1308.

2-(4-((4-Acetylphenoxy)methyl)-1H-1,2,3-triazol-1-yl)-1-moropholinoethanone (8n). Yield: 76%; M.P.: 255°C; brown solid; IR (Neat) ν cm^{-1}: 3329, 3156, 2982, 2916, 2850, 1673, 1661, 1643, 1600, 1421, 1257, 1235, 1177, 1111, 1056, 1042, 848, 820; ^{1}H-NMR (400 MHz, $CDCl_3$): δ 2.56 (s, 3H, -CH_3), 3.56–3.73 (m, 8H, 4x-CH_2 of morpholine), 5.24 (s, 2H, -CH_2), 5.30 (s, 2H, -CH_2), 7.04 (d, J = 8 Hz, 2H, Ar-H), 7.85 (s, 1H, 1,2,3-triazole-H), 7.94 (d, J = 8 Hz, 2H, Ar-H); ^{13}C-NMR (100 MHz, $CDCl_3$): δ 26.6, 42.8, 46.0, 51.0, 62.2, 66.5, 66.8, 114.7, 124.8, 130.8, 162.2, 163.5, 196.9; HRMS (ESI)$^+$ calcd for $C_{17}H_{20}N_4O_4$ [M + H]$^+$: 345.1518 and found 345.1564.

Acknowledgment. The author PSP is very much grateful to the University Grants Commission, New Delhi, for the award of Senior Research Fellowship (SRF).

REFERENCES AND NOTES

[1] Bollu, R.; Banu, S.; Bantu, R.; Gopi Reddy, A.; Nagarapu, L.; Sirisha, K.; Ganesh Kumar, C.; Gunda, S. K.; Shaik, K. Biorg Med Chem Lett 2017, 27, 5158.

[2] (a) Anderson, D. I.; Huges, D. Nat Rev Microbiol 2010, 8, 260; (b) Zheng, X.; Sallum, U. W.; Verma, S.; Athar, H.; Evans, C. L.; Hasan, T. Angew Chem Int Ed 2009, 48, 2148; (c) Lopes, S. M. M.; Novais, J. S.; Costa, D. C. S.; Castro, H. C.; Figueiredo, A. M. S.; Ferreira, V. F.; e Melo, T. M. P.; da Silva, F. D. C. Eur J Med Chem 2018, 143, 1010.

[3] (a) Aufort, M.; Herscovici, J.; Bouhours, P.; Moreau, N.; Girard, C. Bioorg Med Chem Lett 2008, 18, 1195; (b) Pereira, D.; Fernandes, P. Bioorg Med Chem Lett 2011, 21, 510.

[4] (a) Dheer, D.; Singh, V.; Shankar, R. Bioorg Chem 2017, 71, 30; (b) Anand, A.; Naik, R. J.; Revankar, H. M.; Kulkarni, M. V.; Dixit, S. R.; Joshi, S. D. Eur J Med Chem 2015, 105, 194; (c) Kuntala, N.; Telu, J. R.; Banothu, V.; Suresh Babu, N.; Anireddy, J. S.; Pal, S. Med Chem Commun 2015, 6, 1612; (d) López-Rojas, P.; Janeczko, M.; Kubi'nski, K.; Amesty, Á.; Masłyk, M.; Estévez-Braun, A. Molecules 2018, 23, 199; (e) Zhang, Y.; Qiao, R. Z.; Xu, P. F.; Zhang, Z. Y.; Wang, Q.; Mao, L. M.; Yu, K. B. J Chin Chem Soc 2002, 49, 369.

[5] (a) Bock, V. D.; Hiemstra, H.; van Maarseveen, J. H. Eur J Org Chem 2006, 2006, 51; (b) Binder, W. H.; Kluger, C. Curr Org Chem 2006, 10, 1791; (c) Moses, J. E.; Moorhouse, A. D. Chem Soc Rev 2007, 36, 1249.

[6] (a) Shaikh, M. H.; Subhedar, D. D.; Khedkar, V. M.; Jha, P. C.; Khan, F. A. K.; Sangshetti, J. N.; Shingate, B. B. Chin Chem Lett 2016, 27, 1058; (b) Zou, Y.; Zhao, Q.; Liao, J.; Hu, H.; Yu, S.; Chai, X.; Xu, M.; Wu, Q. Bioorg Med Chem Lett 2012, 22, 2959.

[7] (a) Wang, G.; Peng, Z.; Wang, J.; Li, X.; Li, J. Eur J Med Chem 2017, 125, 423; (b) Wang, G.; Peng, Z.; Wang, J.; Li, J.; Li, X. Bioorg Med Chem Lett 2016, 26, 5719; (c) Ashwini, N.; Garg, M.; Mohan, C. D.; Fuchs, J. E.; Rangappa, S.; Anusha, S.; Swaroop, T. R.; Rakesh, K. S.; Kanojia, D.; Madan, V.; Bender, A.; Koeffler, H. P.; Basappa, B. K.; Rangappa, S. Bioorg Med Chem 2015, 23, 6157; (d) Bathula, S. N. P.; Vadla, R. Asian J Pharm Clin Res 2011, 4, 66; (e) Philip, S.; Purohit, M. N.; La, K. K.; Eswar, M. S.; Raizaday, T.; Prudhvi, S.; Pujar, G. V. Int J Pharm Sci 2014, 6, 185; (f) Pokhodylo, N.; Shyyka, O.; Matiychuk, V. Sci Pharm 2013, 81, 663; (g) Majeed, R.; Sangwan, P. L.; Chinthakindi, P. K.; Khan, I.; Dangroo, N. A.; Thota, N.; Hamid, A.; Sharma, P. R.; Saxena, A. K.; Koul, S. Eur J Med Chem 2013, 63, 782.

[8] (a) Pawar, C. D.; Sarkate, A. P.; Karnik, K. S.; Shinde, D. B. Egyp J Bas App Sci 2017, 4, 310; (b) Kulabaş, N.; Tatar, E.; Özakpınar, Ö. B.; Özsavcı, D.; Pannecouque, C.; Clercq, E. D.; Küçükgüzel, İ. Eur J Med Chem 2016, 121, 58.

[9] Shahar, Y. M.; Afroz, B. M.; Siddiqui, A. A.; Abdullah, M. M.; Clercq, E. D. Enzyme Inhib Med Chem 2009, 24, 876.

[10] (a) Emmadi, N. R.; Bingi, C.; Kotapalli, S. S.; Ummani, R.; Nanubolu, J. B.; Atmakur, K. Biorg Med Chem Lett 2015, 25, 2918; (b) Pattan, S. R.; Hullolikar, R. L.; Pattan, J. S.; Kapadnis, B. P.; Dighe, N. S.; Dengale, S. S. J Pharm Sci Res 2009, 1, 63.

[11] Turan-Zitouni, G.; Yurttas, L.; Kaplancikh, Z. A. Med Chem Res 2015, 24, 2406.

[12] Anna Pratima, G. N.; Dipali, D.; Hemant, D. U. Eur J Exp Biol 2012, 2, 343.

[13] (a) Neeraja, P.; Srinivas, S.; Mukkanti, K.; Dubey, P. K.; Pal, S. Bioorg Med Chem Lett 2016, 26, 5212; (b) Rajiv, D.; Devender, P.; Sunita, B. Bull Chem Soc Ethiop 2006, 20, 235; (c) Parikh, K.; Joshi, D. J Chem Soc 2014, 126, 827; (d) Hou, W.; Zhang, G.; Luo, Z.; Li, D.; Ruan, H.; Ruan, B. H.; Su, L.; Xu, H. Bioorg Med Chem Lett 2017, 27, 5382.

[14] Prashant, T.; Lakshmi, R. V.; Naveen, P.; Gurupadaswamy, H. D.; Bushra, B. A. Free Radical Antioxid 2004, 3, s50.

[15] (a) Kumar, R.; Kuar, M.; Bahia, M. S.; Silkari, O. Eur J Med Chem 2014, 80, 83; (b) Lee, K.; Hee Roh, S.; Xia, Y.; Kang, K. W. Bull Kor Chem Soc 2011, 32, 3666.

[16] Bali, A.; Sharma, K.; Bhalla, A.; Bala, S.; Reddy, D.; Singh, A.; Kumar, A. Eur J Med Chem 2010, 45, 2656.

[17] (a) Dhumal, S. T.; Deshmukh, A. R.; Khillare, L. D.; Alkire, M.; Sarkar, D.; Mane, R. A. J Heterocyclic Chem 2017, 54, 125; (b) Dhumal, S. T.; Deshmukh, A. R.; Bhosale, M. R.; Khedkar, V. M.; Nawale, L. U.; Sarkar, D.; Mane, R. A. Bioorg Med Chem Lett 2016, 26, 3646; (c) Tailor, J. H.; Patel, P. C.; Malik, G. M. Indian J Chem 2014, 53B, 1263.

[18] (a) Haval, K. P.; Argade, N. P. Synthesis 2007 2198; (b) Haval, K. P.; Argade, N. P. J Org Chem 2008, 73, 6936; (c) Deore, P. S.; Haval, K. P.; Gadre, S. R.; Argade, N. P. Synthesis 2014, 46, 2683; (d) Shinde, N. V.; Dhake, A. S.; Haval, K. P. Orient J Chem 2016, 32, 515; (e) Shinde, N. V.; Dhake, A. S.; Haval, K. P. Der Pharma Chem 2015, 7, 251.

[19] (a) Katke, S. A.; Amrutkar, S. V.; Bhor, R. J.; Khairnar, M. V. Int J Pharm Sci Res 2011, 2, 148; (b) Xia, S.; Wang, X. H.; Liu, J. Q.; Liu, C.; Chen, J. B.; Zuo, H.; Xie, Y. S.; Dong, W. L.; Shin, D. S. Bull Kor Chem Soc 2014, 35, 1743.

[20] Mancini, I.; Sicurelli, A.; Guella, G.; Turk, T.; Macek, P.; Sepcic, K. Org Biomol Chem 2004, 2, 1368.

[21] (a) Friesner, R. A.; Murphy, R. B.; Repasky, M. P.; Frye, L. L.; Greenwood, J. R.; Halgren, T. A.; Sanschagrin, P. C.; Mainz, D. T. J Med Chem 2006, 49, 6177; (b) Halgren, T. A.; Murphy, R. B.; Friesner, R. A.; Beard, H. S.; Frye, L. L.; Pollard, W. T.; Banks, J. L. J Med Chem 2004, 47, 1750; (c) Friesner, R. A.; Banks, J. L.; Murphy, R. B.; Halgren, T. A.; Klicic, J. J.; Mainz, D. T.; Repasky, M. P.; Knoll, E. H.; Shelley, M.; Perry, J. K.; Shaw, D. E.; Francis, P.; Shenkin, P. S. J Med Chem 2004, 47, 1739.

[22] (a) Collin, F.; Karkare, S.; Maxwell, A. Appl Microbiol Biotechnol 2011, 92, 479; (b) Barrett, J. F.; Bernstein, J. I.; Krause, H. M.; Hilliard, J. J.; Ohemeng, K. A. Anal Biochem 1993, 214, 313; (c) Chatterji, M.; Unniraman, S.; Mahadevan, S.; Nagraja, V. J Antimicrob Chemother 2001, 48, 479.

SUPPORTING INFORMATION

Additional supporting information may be found online in the Supporting Information section at the end of the article.